Enhanced conversion efficiencies for pillar array solar cells fabricated from crystalline silicon with short minority carrier diffusion lengths

Heayoung P. Yoon, Yu A. Yuwen, Chito E. Kendrick, Greg D. Barber, Nikolas J. Podraza et al.

Related Articles

Additional information on Appl. Phys. Lett.

Journal Homepage: http://apl.aip.org/

Journal Information: http://apl.aip.org/about/about_the_journal

Top downloads: http://apl.aip.org/features/most_downloaded

Information for Authors: http://apl.aip.org/authors

Enhanced conversion efficiencies for pillar array solar cells fabricated from crystalline silicon with short minority carrier diffusion lengths

Heayoung P. Yoon,[1,a)] Yu A. Yuwen,[1] Chito E. Kendrick,[2] Greg D. Barber,[3] Nikolas J. Podraza,[1] Joan M. Redwing,[2] Thomas E. Mallouk,[3] Christopher R. Wronski,[1] and Theresa S. Mayer[1,b)]

[1]*Department of Electrical Engineering, The Pennsylvania State University, University Park, Pennsylvania 16802, USA*
[2]*Department of Materials Science and Engineering, The Pennsylvania State University, University Park, Pennsylvania 16802, USA*
[3]*Department of Chemistry, The Pennsylvania State University, University Park, Pennsylvania 16802, USA*

Radial n^+-p^+ junction solar cells composed of densely packed pillar arrays, 25-μm-tall and 7.5 μm in diameter, fabricated from p-type silicon substrates with extremely short minority carrier diffusion lengths are investigated and compared to planar cells. To understand the two times higher AM 1.5 efficiencies of the pillar array cells, dark and light *I-V* characteristics as well as spectral responses are presented for the two structures. The higher pillar array cell efficiencies are due to the larger short-circuit currents from the larger photon absorption thickness and the shorter carrier collection length, with a significant additional contribution from multiple reflections in the structure. © *2010 American Institute of Physics*. [doi:10.1063/1.3432449]

There is growing interest in developing device architectures for enhancing the performance of solar cells fabricated using inexpensive materials that are suitable for cost-effective, large-scale integration.[1,2] Radial p–n junction structures composed of vertically aligned micro- or nanopillar arrays are of interest because they may allow cell fabrication with materials having short minority carrier diffusion length.[3,4] Unlike planar cells, where the light absorption and carrier collection are in competition, the radial junction architecture offers the advantage of decoupling the processes. In this case, cells can be thick in the direction of incident light to maximize absorption of solar radiation, while at the same time being thin in the direction of carrier collection to facilitate efficient extraction of light-generated carriers. Using such a geometry, photoelectrochemical studies on Cd-(Se,Te) showed more efficient carrier collection in nanowire arrays than in planar photoelectrodes.[5] Moreover, recent work indicates that radial junction micro- and nanowires are also promising candidates for low-cost photovoltaics.[6,7]

Pillar array structures can be designed to optimize solar cell efficiency by varying the diameter, the length, and the distance between pillars. Energy conversion efficiencies of various pillar array cells have been estimated theoretically[3,8] and several light trapping strategies have been proposed.[9–11] Recently, Kayes *et al.*[12] studied radial junction arrays fabricated from a lightly doped n-type Si substrate ($\sim 1 \times 10^{15}$ cm^{-3}; 2–8 Ω cm) with a minority carrier diffusion length, $L_n \geq 100$ μm, and reported photovoltaic properties for two different pillar diameters (5 μm, 50 μm) including the effect of increased junction area on open-circuit voltage (V_{oc}). Here, we report a comparison of etched radial n^+-p^+ junction pillar array solar cells and corresponding planar cells that were fabricated using *heavily* doped p-type Si substrates with $L_n \sim 10$ μm and ~ 1 μm.[13] Such short minority carrier diffusion lengths are expected in inexpensive materials such as polysilicon and hot wire-grown Si thin films[14] as well as vapor-liquid-solid grown Si nanowires,[15] which can be integrated onto glass or flexible substrates. Cells with pillar array and planar geometries were characterized with dark and light current-voltage (*I-V*) measurements as well as their spectral response. The direct and quantitative comparison of these cells offers important insight for the design optimization of radial junction pillar array solar cells that are made using emerging low-cost materials and processes.

Hexagonally packed arrays of nominally 7.5 μm diameter and 25 μm tall pillars were etched in p^+ crystalline (100) Si substrates with resistivities of ~ 0.02 Ω cm (A) and <0.005 Ω cm (B), corresponding to doping concentrations of $\sim 5 \times 10^{18}$ cm^{-3} ($L_n \sim 10$ μm) and $\sim 7 \times 10^{19}$ cm^{-3} ($L_n \sim 1$ μm), respectively. The center-to-center distance between the pillars is 10.7 μm, giving a pillar filling fraction of $\sim 38\%$. The pillar array cells were fabricated by defining a SiO$_2$ hard mask using optical lithography and reactive ion etching. The mask pattern was transferred into the p^+ Si substrates using a Bosch deep reactive ion etching (DRIE) process,[16] and the resulting polymeric coating on the pillar sidewalls was removed using an O$_2$ plasma followed by a Piranha (H$_2$SO$_4$:H$_2$O$_2$=1:1) wet clean. The sidewall roughness and damage introduced during DRIE were significantly reduced by incorporating two successive thermal oxidation and strip cycles prior to dopant diffusion, as shown in the inset of Fig. 1(a). After a standard wet chemical clean, n^+-p^+ junctions were formed by gas phase diffusion (1000 °C, 13 min) from phosphorus oxychloride (POCl$_3$), giving a surface doping concentration of $\sim 10^{20}$ cm^{-3} and a junction depth of ~ 0.3 and 0.2 μm in the A and B substrates, respectively. The measured pillar diameters for different devices fabricated on the same p^+ Si substrate varied slightly from 7.3 to 7.8 μm.

To account for edge effects, pillar array solar cells with two different active areas of 2.7×2.7 mm^2 and 5.2×5.2 mm^2 were fabricated and characterized. For both cell areas, the square pillar array was surrounded by a 0.2 mm

a)Electronic mail: hxy148@psu.edu.
b)Electronic mail: tsm2@psu.edu.
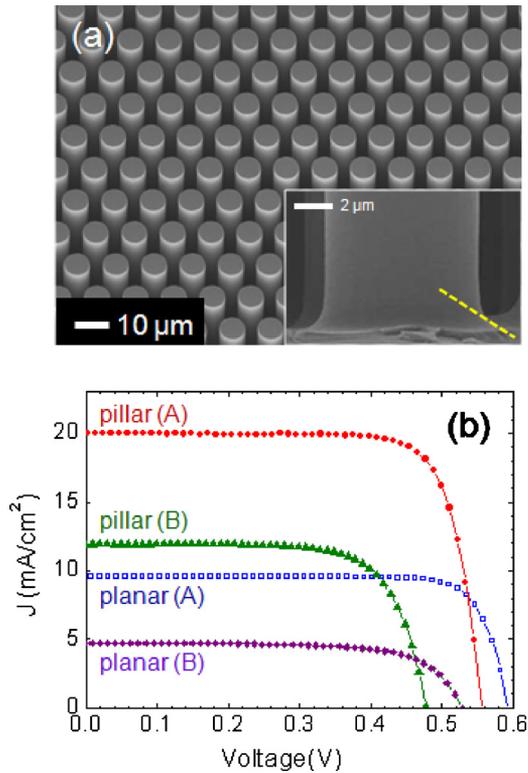
FIG. 1. (Color online) (a) FESEM image of a portion of the 2.7 × 2.7 μm^2 etched radial n$^+$–p$^+$ junction pillar array cell that is composed of ∼10^5 pillars that are 7.5 μm in diameter and 25 μm tall. Inset shows the sidewall profile at the base of a pillar. (b) Light *J-V* characteristics of planar and etched radial junction pillar array solar cells. Sample A is formed by diffusing an n$^+$ junction in a p$^+$ Si substrate with $N_A = 5 \times 10^{18}$ cm^{-3}, L_n ∼ 10 μm while sample B is formed using the same diffusion conditions in a p$^+$ Si substrate with $N_A = 7 \times 10^{19}$ cm^{-3}, L_n ∼ 1 μm.

wide planar junction. Thus, the small area cell has total of ∼10^5 pillars, while the larger area cell has ∼4×10^5 pillars. Ohmic contacts were formed to the backside of the p$^+$ Si substrates by annealing an evaporated Al film. The frontside contacts to the n$^+$ diffused layers were formed with indium dots on the four corners of the cell. Figure 1(a) shows a field emission scanning electron microscope (FESEM) image of a small portion of an etched pillar array cell. The high magnification FESEM image of one pillar, shown as an inset, highlights the region at the base of each pillar. The light *I-V* characteristics of the pillar array and planar cells were measured using a solar simulator with an Air Mass 1.5G (AM 1.5G) source. The external quantum efficiencies (EQEs) were obtained using a broad-spectrum xenon light source and a monochromator.

The light *I-V* characteristics for the small area planar and pillar array solar cells are shown in Fig. 1(b). The cells were illuminated through a 2.7 × 2.7 mm^2 opaque aperture to de-

fine the active area. The efficiencies (η), fill factors (FFs), open-circuit voltages (V_{oc}), and short-circuit current densities (J_{sc}), for cells fabricated using substrates A and B are listed in Table I. As expected, the planar cell efficiencies scale with the minority carrier diffusion length of the p$^+$ substrate, and are 4.6% for substrate A ($N_A = 5 \times 10^{18}$ cm^{-3}, L_n ∼ 10 μm) versus 1.7% for substrate B ($N_A = 7 \times 10^{19}$ cm^{-3}, L_n ∼ 1 μm). The significantly lower efficiency of the planar cell fabricated from the most heavily doped p$^+$ Si substrate is due to all three solar cell parameters being inferior as a consequence of the higher carrier recombination (degrades J_{sc},FF) and the higher J_0 (degrades V_{oc}) of these junctions. In comparison, the pillar array cells have FF and V_{oc} values that are very similar to the corresponding planar devices, indicating that the electrical quality of the etched junctions is comparable to that of the planar junctions. Notably, the factor of 2 higher efficiencies measured for both types of pillar array cells is due to more than a doubling in the J_{sc} from 9.6 to 20 mA/cm^2 for substrate A ($\eta = 8.7\%$) and from 4.7 to 11.7 mA/cm^2 ($\eta = 3.7\%$) for substrate B. The larger area pillar array cell had nearly identical values of J_{sc} and efficiency, which confirms that the observed increase in efficiency is primarily due to light absorption and collection within the pillar array.

The dark current density (*J*)-*V* characteristics obtained on the small area pillar array and planar cells fabricated using substrate A ($N_A = 5 \times 10^{18}$ cm^{-3}) are shown in Fig. 2(a). Both cells show well defined diode characteristics but with significant differences. The planar device has a diode quality factor of $n = 1.1$, while the pillar array has a higher $n = 1.49$. The saturation current density J_0 of the planar device is $J_0 = 3.0$ pA/cm^2, which is much lower than the pillar array $J_0 = 0.9$ nA/cm^2. The reverse bias leakage current is nearly voltage independent for the planar device but varies roughly as the square root of voltage for the pillar array device. These differences all point to the lower electrical quality of n$^+$–p$^+$ junctions in the pillar array cells, possibly due to residual sidewall damage introduced by the DRIE process. Nevertheless, as shown in Table I, the V_{oc} values are quite similar because the increase in J_{sc} from the pillar array architecture offsets the reduction in V_{oc} due to the increase in J_0. Not unexpectedly, as summarized in Table I, the diode properties of the planar and pillar array cells fabricated using substrate B ($N_A = 7 \times 10^{19}$ cm^{-3}) are inferior to those of substrate A, with higher values of n, J_0, and reverse bias leakage. The degradation in diode properties together with the lower values of J_{sc} explains the correspondingly lower efficiency for these cells.

The EQEs for the small area planar and pillar array solar cells fabricated using substrate A (5×10^{18} cm^{-3}) are shown in Fig. 2(b). The integration of the quantum efficiencies with

TABLE I. Photovoltaic properties of the 2.7 × 2.7 mm^2 active area planar and pillar array cells. Sample A is formed using a p$^+$ Si substrate with $N_A = 5 \times 10^{18}$ cm^{-3}, L_n ∼ 10 μm while sample B is formed using a p$^+$ Si substrate with $N_A = 7 \times 10^{19}$ cm^{-3}, L_n ∼ 1 μm.

Device	n	J_0 (nA/cm^2)	$I_{0,cell}$ (nA)	J_{sc} (mA/cm^2)	V_{oc} (V)	FF (%)	Efficiency (%)
A (planar)	1.08	0.003	0.0002	9.6	0.59	80.8	4.6
A (pillar)	1.49	0.90	0.4	20.0	0.56	78.1	8.7
B (planar)	1.54	0.8	0.06	4.7	0.53	71.5	1.7
B (pillar)	1.72	22.0	10.3	11.7	0.48	71.4	3.7
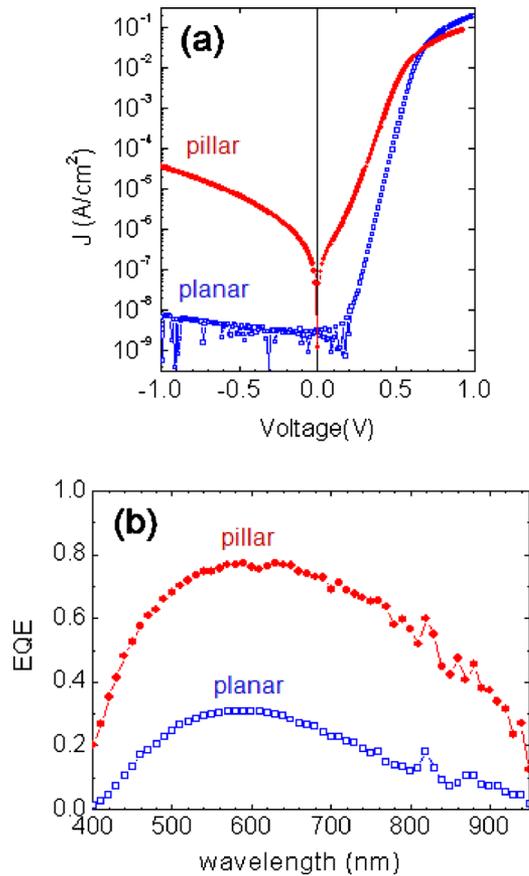
FIG. 2. (Color online) (a) Dark *J-V* characteristics and (b) EQEs of a 2.7 ×2.7 mm² active area planar and an etched radial junction pillar array solar cell fabricated using the p⁺ Si substrate with $N_A = 5 \times 10^{18}$ cm⁻³, L_n ∼10 μm (sample A).

AM 1.5G spectra[17] confirmed the measured J_{sc} values determined from the light *I-V* measurements (Table I). Specifically, assuming a specular reflection at each planar Si/air interface and no absorption of the light reflected at the base of the pillars, ∼9 mA/cm² of the total 20 mA/cm² can be attributed to the absorption of light incident on the top planar surface of the pillars (38% of the active area, complete collection of photogenerated carriers in the pillar), with an additional ∼4 mA/cm² that arises from the planar surfaces at the base of the pillars and at the edges of the cell (62% of active area). These two contributions account for a maximum of ∼13 mA/cm² of the measured light current.

A more detailed optical analysis of the pillar array cell indicates that the additional ∼7 mA/cm² light current can be attributed to multiple specular reflections within the structure. As shown in the inset of Fig. 1(a), the DRIE process used to fabricate the array creates a ledge around the base of the pillars at an angle of ∼30° relative to the planar surface. Importantly, the shallow slope of this ledge reflects normally incident light onto nearby pillars, where a fraction of light is absorbed. The reflected light that is not initially absorbed in the pillar as well as the light that escapes the pillar at each reflection can be absorbed in the adjacent pillars in subsequent reflections until it is scattered out of the structure. These multiple reflections lead to an effective absorption length much greater than 25 μm. Thus, the contribution from the multiple reflections within the pillars and between adjacent pillars results in similar behavior to optical en-

hancement observed in other high-aspect-ratio cell structures.[9,18]

In summary, planar and pillar array solar cells were fabricated using p⁺ crystalline Si substrates with short minority carrier diffusion lengths of $L_n \sim 10$ μm and 1 μm. In both cases, more than a twofold increase in the AM 1.5 conversion efficiency was measured for the radial n⁺–p⁺ junction Si pillar array solar cells as compared to the corresponding planar cells. The large improvement in efficiency of the pillar array cells with values of V_{oc} and FF that are comparable to the planar cells is due to the much higher values of J_{sc}. The primary factors that contribute to the higher J_{sc} are the increase in the effective absorption length of the light that is incident on the top planar surface of the pillars as well as the additional contribution from multiple reflections within the pillar array structure. These results demonstrate that the radial junction pillar array architecture is effective for enhancing the conversion efficiency of solar cells fabricated using cost-effective materials and fabrication processes. Further optimization of the pillar array design (e.g., diameter, height, filling geometry, and fraction) for Si with short $L_{n,p}$ is expected to give even larger improvements in cell performance.

[1]M. A. Green and S. R. Wenham, Appl. Phys. Lett. **65**, 2907 (1994).
[2]L. Y. Cao, J. S. White, J. S. Park, J. A. Schuller, B. M. Clemens, and M. L. Brongersma, Nat. Mater. **8**, 643 (2009).
[3]B. M. Kayes, H. A. Atwater, and N. S. Lewis, J. Appl. Phys. **97**, 114302 (2005).
[4]Z. Y. Fan, D. J. Ruebusch, A. A. Rathore, R. Kapadia, O. Ergen, P. W. Leu, and A. Javey, Nano Res. **2**, 829 (2009).
[5]J. M. Spurgeon, H. A. Atwater, and N. S. Lewis, J. Phys. Chem. C **112**, 6186 (2008).
[6]S. W. Boettcher, J. M. Spurgeon, M. C. Putnam, E. L. Warren, D. B. Turner-Evans, M. D. Kelzenberg, J. R. Maiolo, H. A. Atwater, and N. S. Lewis, Science **327**, 185 (2010).
[7]E. C. Garnett and P. D. Yang, J. Am. Chem. Soc. **130**, 9224 (2008).
[8]Z. Y. Fan, H. Razavi, J. W. Do, A. Moriwaki, O. Ergen, Y. L. Chueh, P. W. Leu, J. C. Ho, T. Takahashi, L. A. Reichertz, S. Neale, K. Yu, M. Wu, J. W. Ager, and A. Javey, Nat. Mater. **8**, 648 (2009).
[9]M. D. Kelzenberg, M. C. Putnam, D. B. Turner-Evans, N. S. Lewis, and H. A. Atwater, Proceedings of the 34th IEEE Photovoltaic Specialists Conference, 2009, pp. 001948–001953.
[10]J. S. Li, H. Y. Yu, S. M. Wong, G. Zhang, X. W. Sun, P. G. Q. Lo, and D. L. Kwong, Appl. Phys. Lett. **95**, 033102 (2009).
[11]J. Rybczynski, K. Kempa, A. Herczynski, Y. Wang, M. J. Naughton, Z. F. Ren, Z. P. Huang, D. Cai, and M. Giersig, Appl. Phys. Lett. **90**, 021104 (2007).
[12]B. M. Kayes, M. A. Filler, M. D. Henry, J. R. Maiolo III, M. D. Kelzenberg, M. C. Putnam, J. M. Spurgeon, K. E. Plass, A. Scherer, N. S. Lewis, and H. A. Atwater, Proceedings of the 33rd IEEE Photovoltaic Specialists Conference, 2008, pp. 1–5.
[13]M. S. Tyagi and R. Vanoverstraeten, Solid-State Electron. **26**, 577 (1983).
[14]R. Bruggemann, J. P. Kleider, C. Longeaud, D. Mencaraglia, J. Guillet, J. E. Bouree, and C. Niikura, J. Non-Cryst. Solids **266–269**, 258 (2000).
[15]M. C. Putnam, D. B. Turner-Evans, M. D. Kelzenberg, S. W. Boettcher, N. S. Lewis, and H. A. Atwater, Appl. Phys. Lett. **95**, 163116 (2009).
[16]M. D. Henry, S. Walavalkar, A. Homyk, and A. Scherer, NANO **20**, 255305 (2009).
[17]Web site for NREL's AM1.5 Standard Dataset: http://rredc.nrel.gov/solar/spectra/am1.5/.
[18]J. Zhu, Z. F. Yu, G. F. Burkhard, C. M. Hsu, S. T. Connor, Y. Q. Xu, Q. Wang, M. McGehee, S. H. Fan, and Y. Cui, Nano Lett. **9**, 279 (2009).